Available online at www.sciencedirect.com

ScienceDirect

Procedia CIRP 46 (2016) 115 – 118

www.elsevier.com/locate/procedia

7th HPC 2016 – CIRP Conference on High Performance Cutting

Effects of different levels of abstraction simulating heat sources in FEM considering drilling

Patrick Bollig[a]*, Dominik Köhler[a], Frederik Zanger[a], Volker Schulze[a]

[a]*wbk Institute for Production Science, Kaiserstraße 12, Karlsruhe 76131 Germany*

* Corresponding author. Tel.: +49-721-608-42450; fax: +49-721-608-45004. *E-mail address:* Frederik.Zanger@kit.edu

Abstract

This paper presents a comparison of three different methods of simulating heat sources in 3D-FEM-simulations with various levels of abstraction for drilling. The investigated methods are modelled and evaluated with respect to calculation time and accuracy of simulated temperature fields and phase transformations. Results are showing a significant variance of the maximum temperature and temperature distribution for the three different heat sources although the same amount of energy is used in the simulation model. According to the longest simulation time the most detailed heat source provides a realistic temperature distribution.

Peer-review under responsibility of the International Scientific Committee of 7th HPC 2016 in the person of the Conference Chair
Prof. Matthias Putz

Keywords: Finite element method (FEM); Drilling; Modelling

Nomenclature

f	feed rate [mm]
r	radius [mm]
t	time [s]
T	temperature [°C]
v_c	cutting speed [mm/min]

1. Introduction

The last several years showed an immensely increased usage of simulations for predicting thermal effects in machining. Simulation results of three different types of heat sources were compared to experimental results [1]. These three heat sources differ in duration and magnitude but the amount of heat flux applied in the 3D drilling simulation stays the same. The results show that it leads to excessively high maximum temperatures when the total heat flux is applied in only one second. An application of the heat flux for the whole process time at a low magnitude only heats the workpiece and does not reflect the experimental temperatures. The best accordance to experimental data showed a step by step heating of the workpiece where the total heat flux was divided into four loading steps.

Biermann et al. modeled the heat input in a 3D-FEM deep drilling simulation by using discrete segmentation of the drilling hole. Different segmentation sizes were used to model their influence on the resulting temperature distribution. The moving heat source was dependent on the process parameters. Results show convergent behavior for segment sizes close to the feed per tooth values and increased maximum temperatures for big segmentation sizes [2].

A 3D FEM simulation model is presented in [3] talking into account the complete kinematics of the drilling process. The heat input was implemented as a nodal boundary condition and considers the feed rate and the rotation of the drilling tool. Empirical equations were used to model the temperature distribution at the main cutting edge and the minor cutting edge. The heat input due to material removal was also included. This method shows very good agreement with experiments for the temperature distribution data as well as the prediction of phase transformations.

Considering the different types of modeling heat sources in FEM simulations the focus is on the description of deformation forces and temperature [1-3]. However there is no indication of

Peer-review under responsibility of the International Scientific Committee of 7th HPC 2016 in the person of the Conference Chair
Prof. Matthias Putz
doi:10.1016/j.procir.2016.03.186

which abstraction type is useful to effectively simulate phase transformations. For this reason, the presented work aims at characterizing three different types of heat sources and their accuracy in predicting temperature distribution and phase transformation for different levels of abstract heat sources.

2. Modeling and simulation of heat sources in drilling

The following sections will introduce the modelling approach for the comparison of three different types of heat sources for drilling simulations. A closer look is taken at the 3D-FEM simulation, the modeling of phase transformations and the temperature generation.

2.1. 3D-FEM-simulation-model

The developed 3D FEM simulation model was created using the software ABAQUS/Standard and describes the kinematics of a drilling process with three different levels of abstract heat sources.

It represents a first step by bringing the 3D drilling simulation introduced in [3] to a more complex workpiece geometry with increased thermo-mechanical loading efficiency. This optimization step is inevitable for the prospective compensation of thermally caused distortion during drilling and fast simulation times. Increasing efficiency became necessary due to long simulation times of the model presented in [3].

Within this new simulation model, no forces have been modeled so far, because the focus in this work is on describing the temperature field and predicting phase transformations. All the associated work is presented in the following sections, in order to find the best and most efficient heat source for the calculation of phase transformations.

The implemented material model for AISI 4140 is the same as the one established in [4]. Temperature dependent parameters are used such as specific heat, elasticity, density or conductivity. The deformation behavior is based on an isotropic model created by Vöhringer and Voce with a yield criterion according to von Mises [5].

For the simulation of phase transformations, a special meshing strategy becomes necessary. It is shown in [4] that phase transformations in the form of white layers appear on the surface of AISI 4140 with a thickness of only a few micrometers. So the FEM-mesh needs to be adjusted to this transformation size to enable a good scale for graphical exposure. For this reason, a mesh refinement is used going from the central point to the wall surface of the drilled hole. A small circle next to the surface of the drilling hole is meshed with a high element density. The border area of the workpiece is meshed with a very rough mesh to save the number of elements.

Several types of boundary conditions are modeled in the simulation. The whole model is covered by a heat transfer boundary condition due to radiation. This parameter is set to a value of 20 W/m²*K. Furthermore, the 3-Point jaw chuck system in the machine tool is represented by reducing some degrees of freedom in the model as a boundary condition.

2.2. Modeling of phase transformations

In the presented work, the kinetics of the transformation and the short time austenization is considered the main mechanism of phase transformation. The transformation process is split into a diffusion controlled and a diffusionless transformation. A modified phenomenological approach by Avrami [6] is used to describe the austenitization process and retransformation to ferrite/perlite or bainite [7]. The diffusionless transformation, also called martensitic transformation, is considered by the equations of Koistinen and Marburger [8, 9] as a modified approach of Skrotzki [10]. This modeling approach is presented in [11] and shows good agreement to experimental results. This good relation between the heating rates and the austenitization is the basis of a proper calculation of the induced phase transformation particularly for different local thermal loads [4, 11].

2.3. Modelling different types of heat sources for drilling

For the simulation of thermal effects in machining operations, many different types of modelling approaches for the heat or temperature input in FEM simulations exist. In this work, the heat generation is not caused by a heat flux but by a temperature boundary condition. This temperature boundary condition is used to load selected nodes at the surface in the FEM mesh of the simulated part. This method was chosen since for simulating phase transformations, a close temperature fit from simulation results to the experimentally measured temperatures is of particular importance. Phase transformations will occur when the austenite starting temperature and a subsequent critical cooling rate is exceeded. For this description, it is more accurate to use numerically found time dependent temperature equations as boundary conditions than heat fluxes. In this case, by applying temperatures directly to the FEM mesh, the measured temperatures and maximum temperatures are not exceeded and stay close to the measured values. In this work, the validated equation for the main cutting edge used in [4] is implemented into the simulation model:

$$T(r, v_c, f, t) = 170.4 \cdot r^{0.23} \cdot {v_c}^{0.23} \cdot f^{0,12} \cdot t^{0.05} \quad (1)$$

This temperature T equation is based on experimental data and was harmonized via regression approaches dependent on the drill radius r, the cutting speed v_c, the feed rate f as well as the drilling time t. In Fig. 1, a graphical exposure of equation 1 is given for v_c = 300 m/min and f = 0.3 mm.

The first heat source model represents the drilling process in a very abstract way. In this kind of heat source, the drilling hole is already part of the simulation model and the temperature is loaded as a node set on the surface of the drilling hole, cf Fig. 2. To consider the drilling process and its kinematics, the drilling hole is divided into annular segments over the complete drilling depth. These annular segments correspond in their thickness and load duration to the feed rate of the drilling tool. So the annular temperature loading on the wall surface of the drilling hole is able to follow the kinematics of the feed rate.

In this case, the temperature loading on the wall surface does not consider the whole experimentally found temperature equation but only the values existing on the surface, cf. Fig. 2.

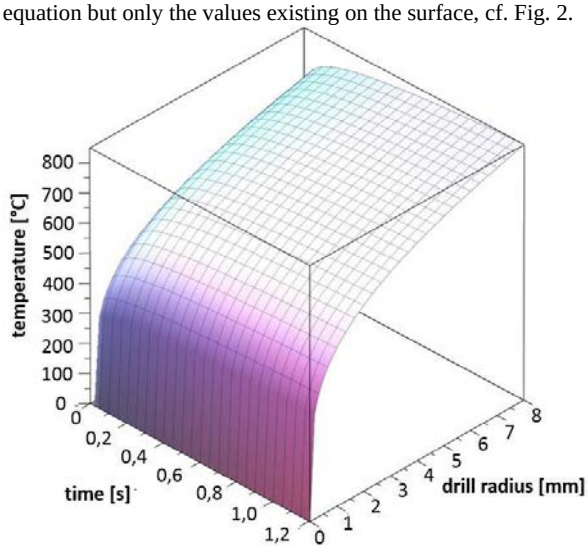

Fig. 1. Analytical temperature distribution using equation (1) for v_c = 300 m/min and f = 0.3 mm

The shape of the second heat source model is based on conical segments with an interior angle of 130 degree. This angle is used with regard to the point angle of the drilling tools in the upcoming experimental validation. Identically to the first heat source model, the second heat source model also considers the kinematics of the feed rate. The material removal process is divided into two steps. In the first step, every segment is loaded with the temperature distribution from equation 1. In the second step, the loaded segment is deactivated.

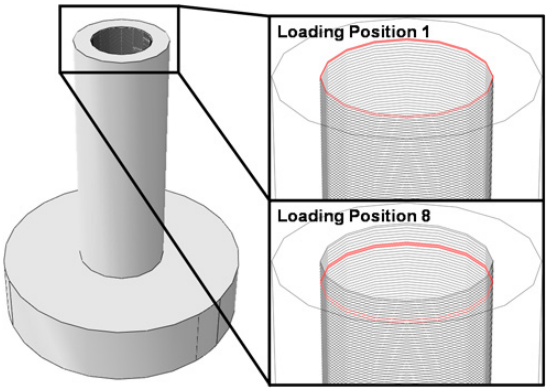

Fig. 2. Different loading positions for the first heat source model of drilling

According to the amount of segments (influences the thickness of the segments) the used time-step for each loading is considering the feed rate of the drilling tool, cf. Fig. 3. Considering the whole kinematics of the drilling process, the third heat source model represents the model that is closest to the drilling process. Having regard to the feed rate, material removal and the rotation of the drilling tool, a complex modelling approach is required, cf. Fig. 4.

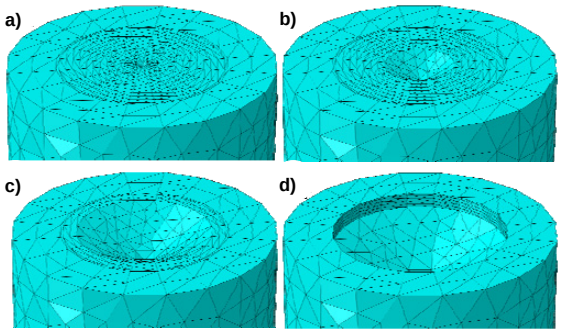

Fig. 3. Material removal process for the second drilling heat source model

The cone-shaped discs of the second heat source model are additionally circular divided into 12 parts (cf. Fig. 4b). The drilling mechanism is again separated into a loading and a deactivation step. In contrast to the second heat source model, only the circular divided and its opposite part, following the rotation of the drilling tool, are loaded and deactivated. This rotation speed and disc thickness is adapted to the cutting speed and the feed rate of the drilling. After a full rotation of the drilling tool the cone-shaped disc is fully removed and the next disc is loaded again in a similar way.

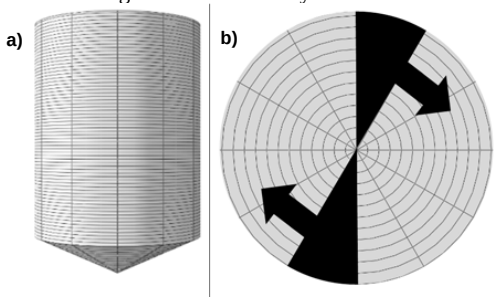

Fig. 4. (a) Segmented drilling hole; (b) schematic circular segmentation for the third heat source model

3. Results of three abstract heat sources

The simulation results of the three modeled abstract heat sources are presented in the following sections under the aspect of their applicability of temperature distribution and prediction for phase transformations.

3.1. Temperature distribution

The simulation results for the temperature distributions are shown in Fig. 5. It can be seen that the second heat source model has a very large area in the drilling hole with high temperatures, compared to the other two models. The main reason for this temperature distribution is based on the type of the heat source itself. There is a heat accumulation due to the constant segment loading, which not appears in the other heat source models. Compared to the third heat source model, the

whole segment is loaded with the temperature equation and not only a part of this segment. The most realistic third heat source model can cool down, while the heat source is moving, considering that the heat input is the same like in the second heat source model. For this reason the third heat source model represents the loading due to the main cutting edge very well, Fig. 5c). As already mentioned the max. temperature is the smallest of all three heat source models, caused by the best modulation of the drilling kinematics. The first heat source model shows the temperature distribution due to a circular loading on the wall surface of the drilling hole, Fig. 5a). It can clearly be seen that the temperature loading due to the circular loading is also visible on the surface of the workpiece. The second heat source model shows this effect once more enhanced attributed to the appearing heat accumulation.

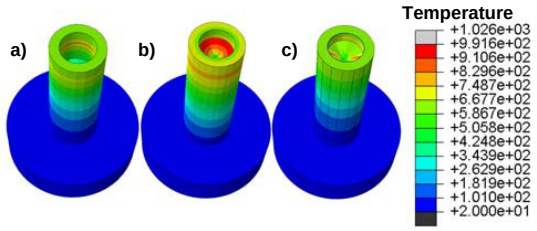

Fig. 5. Simulation results for the temperature distribution (a) first heat source model (b); second heat source model; (c) third heat source model for v_c = 300 m/min and f = 0.3 mm

Fig. 6 shows a comparison of the maximum temperatures calculated in the simulations. The second heat source model has the highest max. temperature, because of the highest amount of total heat input. The lowest max. temperature can be found in the third heat source model according to the best modulation of the drilling kinematics.

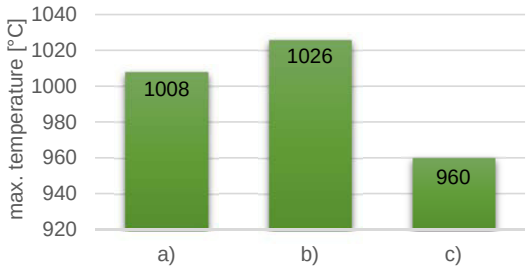

Fig. 6. Comparison of the maximum temperatures [°C] for a) first heat source, b) second heat source and c) third heat source

3.2. Phase transformation

The simulation results for the prediction of phase transformations show similar behavior for the volume amount of transformed martensite due to the connection to the max. temperatures. The smallest and probably most realistic volume amount of martensite can be seen in Fig. 7, for the third heat source model, according to a metallurgical analysis of a similar workpiece with a little smaller drilling hole. This volume amount of transformed martensite increases applying the first model and is maximal using the second model.

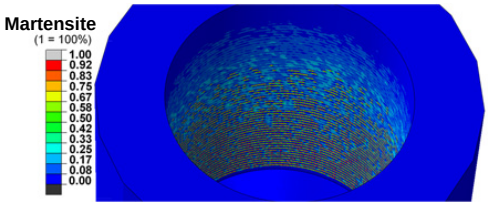

Fig. 7. Calculated volume amount of martensite for third heat source model

4. Conclusions

The results show a great influence on the temperature distribution and phase transformation according to the used level of abstract heat source. The closest approach to the drilling process shows the most realistic simulation results, but needs the highest simulation time. The difference in simulation time is about factor 10 for the third heat source model compared to the first heat source model. In Future work the simulation results have to be verified by experimental data and the simulation will be enlarged with further drilling holes.

Acknowledgements

The authors gratefully thank the German Research Foundation for the support of the priority program 1480.

References

[1] Pabst R. Mathematische Modellierung der Wärmestromdichte zur Simulation des thermischen Bauteilverhaltens bei der Trockenbearbeitung. Forschungsberichte aus dem wbk Institut für Produktionstechnik. Shaker Verlag Aachen. Dissertation. Universität Karlsruhe (TH); 2008

[2] Biermann D, Iovkov I. Modeling and simulation of heat input in deep-hole drilling with twist drills and MQL. Procedia CIRP (8); 2013. p. 88-93

[3] Schulze V, Zanger F, Michna J, Lang F. 3D-FE-Modelling of the Drilling Process – Prediction of Phase Transformations at the Surface Layer. Procedia CIRP (8); 2013. p. 33-38

[4] Michna J. Numerische und experimentelle Untersuchung zerspanungsbedingter Gefügeumwandlungen und Modellierung des thermo-mechanischen Lastkollektivs beim Bohren von 42CrMo4. Forschungsberichte aus dem wbk Institut für Produktionstechnik. Shaker Verlag Aachen. Dissertation; 2014

[5] Autenrieth H. Numerische Analyse der Mikrozerspanung am Beispiel von normalisiertem C45E. Dissertation, Universität Karlsruhe (TH); 2010

[6] Mioković T, Schulze V, Vöhringer O, Löhe D. Prediction of phase transformations during laser surface hardening of AISI 4140 including the effects of inhomogeneous austenite formation. Mater.Sci.Eng. (435/436a); 2006. p. 547-555

[7] Schulze V, Michna J, Zanger F, Faltin C, Maas U, Schneider J. Influence of cutting parameters, tool coatings and friction on the process heat in cutting processes and phase transformations in workpiece surface layers. J. Heat Treatm. Mat. 68; 2013. p. 22-29

[8] Koistinen DP, Marburger RE. A genereal equation prescribing the extent of the austenite-martensite transformation in pure iron-carbon alloys and plain carbon steels. Acta Metall (7); 1959. p. 59-60

[9] Mioković T, Schulze V, Löhe D, Vöhringer O. Experimentelle Analyse und Modellierung des Kurzzeitumwandlungsverhaltens von Stählen am Beispiel von 42CrMo4. HTM Haerterei-Techn. Mitt (53); 2003. p.1-10

[10] Skrotzki B. The course of the volume fraction of martensite vs. temperature function Mx(T). J. Phys. IV; 1991. P 367-372

[11] Schulze V, Michna J, Zanger F, Pabst R. Modeling the process-induced modifications of the microstructre of work piece surface zone in cutting processes. Adv. Mat. Res (223); 2011. p. 371-380